Chapter VII

RESULTS AND DISCUSSION

VII.A. Summary of the CDG Analysis

Table VII.1 summarizes the optimized CDG data selections used to generate and subsequently extrapolate the VGC to determine the CDG count rates in each energy bin.

Table VII.1 Summary of the CDG data selections.

Energy (MeV)	Data	Data selection for VGC extrapolation
0.8–1.2	P23a	1gToF phi 6–38˚ – (24Na+28Al+22Na+40K+1.4Gaus)
1.2–1.8	P23a	1gToF phi 6–38˚ – (24Na+28Al+22Na+40K+1.4Gaus)
1.8–2.7	P23a	1gToF phi 22–38˚ – 24Na
2.7–4.2	P23a	1gToF phi 22–38˚ – 24Na
4.2–6	P15VSGP	2gToF phi 22–38˚
6–9	P15VSGP	2gToF phi 22–38˚
9–12	P15VSGP	1gToF phi 6–38˚
12–17	P15VSGP	1gToF phi 6–38˚
17–30	P15VSGP	1gToF phi 7–22˚

Table VII.2 The COMPTEL CDG flux and its statistical and systematic errors.

Energy (MeV)	CDG flux	statistical error	systematic error	total error
	(photons/cm^2-s-sr-MeV)			
0.8–1.2	0.00465	0.0011	0.0039	0.0039
1.2–1.8	0.0020	0.00046	0.00105	0.00105
1.8–2.7	0.00121	0.00029	0.00034	0.00044
2.7–4.2	0.000245	0.000123	0.000086	0.00015
4.2–6	6.88e-5	2.43e-5	3.47e-5	4.24e-5
6–9	2.88e-5	1.32e-5	1.34e-5	1.88e-5
9–12	1.88e-5	3.83e-6	2.93e-6	4.82e-6
12–17	11.13e-6	2.11e-6	2.27e-6	3.10e-6
17–30	2.77e-6	1.03e-6	1.20e-6	1.58e-6

Table VII.2 contains the resulting CDG flux values using the Exponential-ToF model, its 1σ statistical and systematic uncertainties. The total error is the quadratic sum of the statistical and systematic errors. Above 1.8 MeV, the systematic errors are comparable to the statistical

uncertainties in the measured CDG flux. However, the systematic errors dominate the 0.8–1.2 and 1.2–1.8 MeV measurements, in particular those associated with the ToF-fit models. We take the mean value of the flux derived using both ToF-fit models as the best representation of the CDG spectrum in the 0.8–1.2 and 1.2–1.8 MeV bins.

VII.B. The Cosmic Diffuse Gamma-Ray Spectrum

The CDG spectrum with the total uncertainties are plotted in figure VII.1. The best fit power-law (described below) is also plotted in figure VII.1 together with the results from some of the pre-COMPTEL experiments. The pre-COMPTEL measurements are those of Trombka et al. (1977) using the gamma-ray spectrometer flown on the Apollo flights labeled *APOLLO*, Schönfelder et al. (1980) using the MPE-balloon Compton telescope labeled *MPE-balloon*, and White et al. (1977) using the UCR-balloon Compton telescope labeled *UCR-balloon*.

The CDG flux measurements in the 1 to 10 MeV range are about 5–10 times lower than the pre-COMPTEL estimates (figure VII.1). The CDG measurements show no evidence of the MeV bump in the 1 to 10 MeV range. The integrated flux from 0.8 to 9 MeV is $(4.7 \pm 1.7) \times 10^{-3}$ photons/cm^2-s-sr and that from 9 to 30 MeV is $(1.5 \pm 0.3) \times 10^{-4}$ photons/cm^2-s-sr. This represents the first significant detection (statistical significance of 7.2σ) of the CDG emission in the 9 to 30 MeV range. The preliminary COMPTEL CDG estimates reported earlier are in good agreement with these results (Kappadath et al. 1995; 1996; 1997) (see figure VII.2).

The COMPTEL CDG spectrum is fit to power-law function, $A \times (E/E_0)^{-\alpha}$, where A is the flux normalization, E is the photon energy, E_0 is taken to be 5 MeV (the logarithmic-midpoint energy between 0.8 and 30 MeV) and α is the spectral index. The resulting differential photon spectrum from 800 keV to 30 MeV is well described ($\chi^2_\nu = 0.43$) by a photon spectral index of -2.4 ± 0.2 and a flux normalization of $(1.05 \pm 0.2) \times 10^{-4}$ photons/cm^2-s-sr-MeV at 5 MeV.

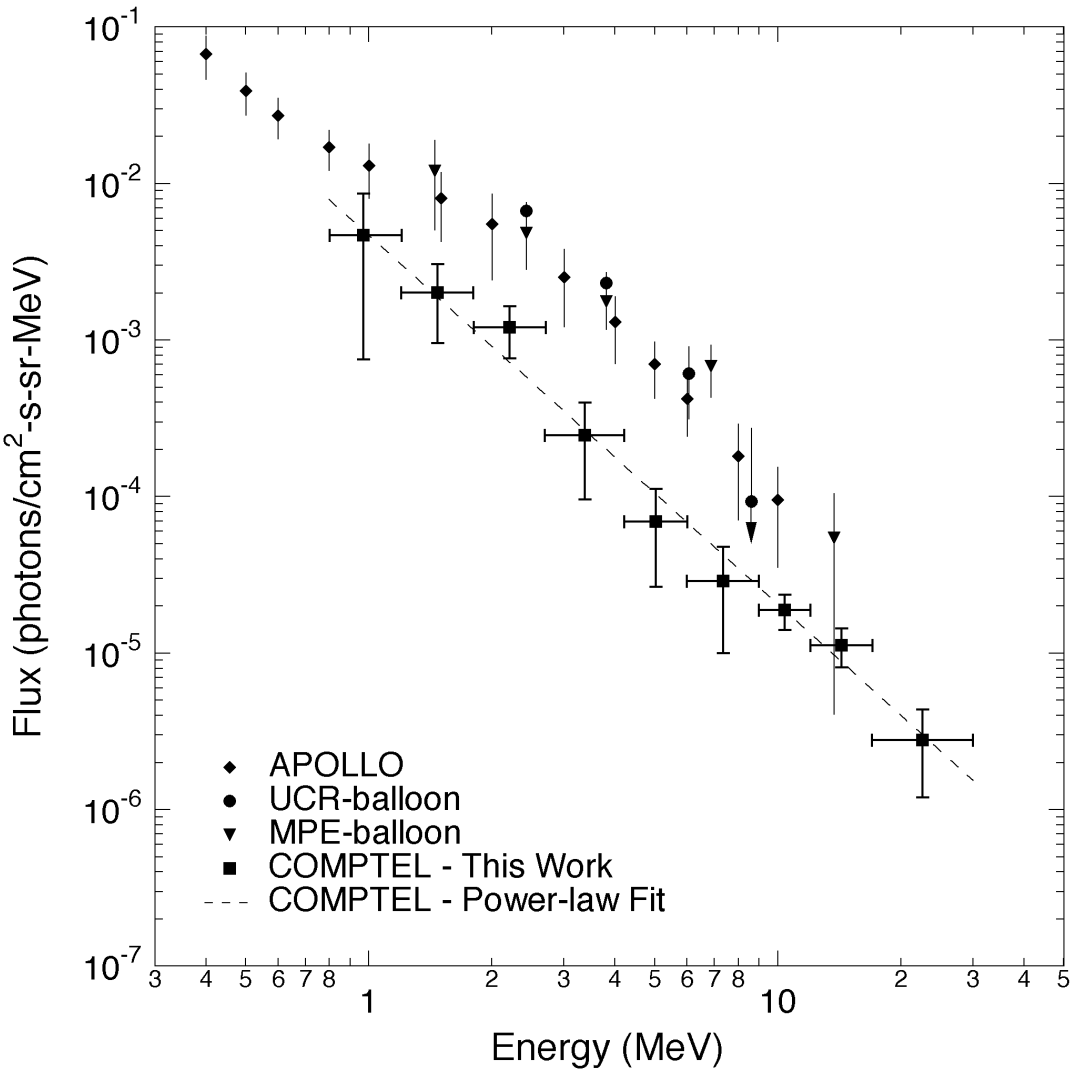

Figure VII.1 The COMPTEL CDG spectrum with the power-law fit together with the results from pre-COMPTEL experiments.

It is important to note that although the CDG spectral results are high latitude measurements, they do *include* contributions from the diffuse Galactic radiation and gamma-ray point sources in the field-of-view. To eliminate the point sources (typically AGNs) one must determine their intensities during the CDG measurements. Out of the 8 AGNs detected by COMPTEL only two AGNs reside in the Virgo Observations, namely, 3C 273 and 3C 279. Assuming a time-averaged spectrum as measured by Hermsen et al. (1993) their combined contributions are <1% at 1 MeV to <4% at 15 MeV, a negligible contribution. One could also use the EGRET AGN detections and estimate their contributions to the CDG emission <30 MeV. However, the spectral and temporal behavior of these AGN below 30 MeV is uncertain.

Therefore, *no* correction for gamma-ray point sources has been included in the COMPTEL CDG spectrum.

The contributions from the diffuse Galactic emission may also contribute to the CDG spectrum even at these high latitudes. The high-latitude diffuse emission is primarily from the bremsstrahlung and inverse-Compton processes. Measurements of the diffuse Galactic emission between 1 and 30 MeV are uncertain because of large uncertainties in the instrumental background in image space and because of uncertainties in the low-energy cosmic-ray electron spectrum and the interstellar radiation field. Therefore, the diffuse Galactic emission is also *not* subtracted from the COMPTEL CDG spectrum. A rough calculation of the diffuse Galactic emission from the Virgo direction using the model of Strong and Youssefi (1995; Strong 1996) (figure VII.2) predicts a contribution to the CDG flux of <5% at 1 MeV, <19% at 3 MeV, <22% at 10 MeV and <35% at 22 MeV (A. Strong, private communication). As a corollary, the CDG measurements place an absolute limit on the diffuse Galactic emission at high latitudes.

Kinzer et al. (1997) determined the cosmic diffuse radiation in the 100–400 keV band using the HEAO-1 A4 MED instrument. The spectrum is fit with a power-law giving a spectral index of -2.75 ± 0.08. Their data are labeled *HEAO-1* in the following figures. More recent measurements of the CDG spectrum from 300 keV to 7 MeV with the SMM/GRS instrument (Watanabe 1996; K. Watanabe, private communication) obey a power-law with a spectral index of -2.90 ± 0.02. Their data are labeled *SMM* in the following figures. The COMPTEL measurements are compatible with the continuation of both these measurements to higher energies (figure VII.2). The HEAO-1 power-law extrapolation follows the upper curve of the SMM results.

The diffuse extragalactic spectrum from 30 MeV to 100 GeV energy range measured with the EGRET instrument (Sreekumar et al. 1998) are labeled *EGRET*. Their results also obey a power-law spectrum with an index of -2.10 ± 0.03. The COMPTEL spectrum is also compatible with the continuation of the diffuse extragalactic spectrum from higher energies (figure VII.2).

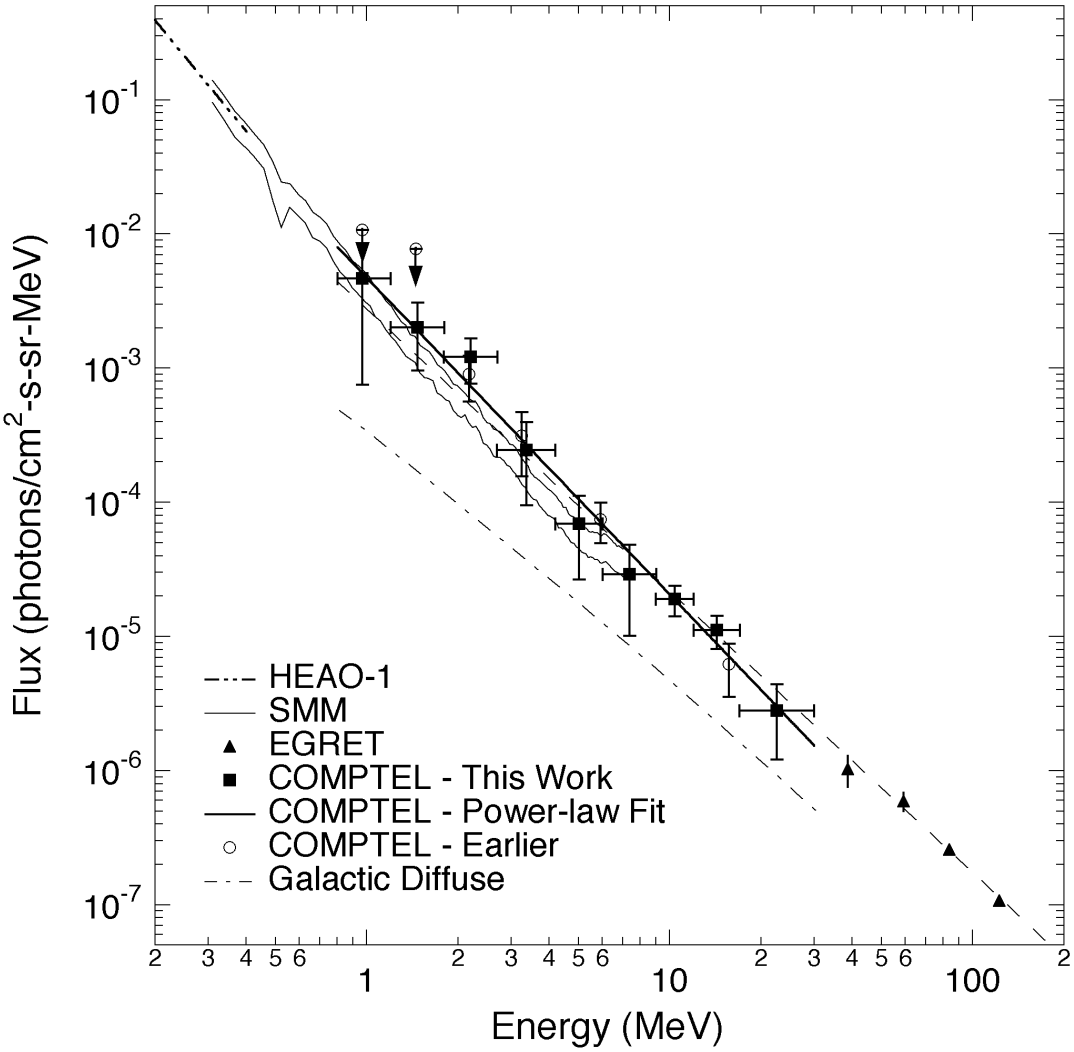

Figure VII.2 The COMPTEL CDG spectrum compared to the results from SMM and extrapolation from EGRET.

The COMPTEL CDG spectrum is therefore compatible with the continuation of all recent CDG data at lower and higher energies. The COMPTEL CDG photon spectral index of –2.4 in the 0.8–30 MeV energy range is of an intermediate value between the steeper slope (–2.9) at lower energies and the harder slope (–2.1) at higher energies. The diffuse spectrum evolves from a soft to hard spectrum in the COMPTEL energy range (see figure VII.3). The *HEAO-1* reference in figures VII.3 and VII.9 include the data of Gruber (1992) and Kinzer et al. (1997).

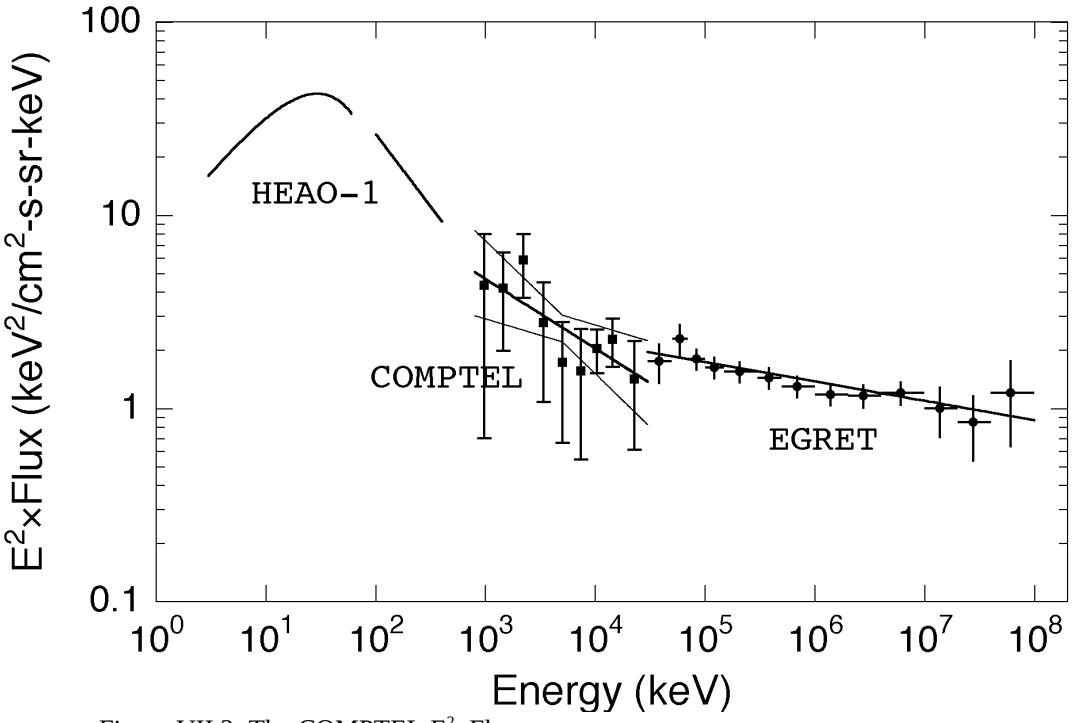

Figure VII.3 The COMPTEL E^2×Flux spectrum.

VII. C. The MeV Bump

The MeV bump, we believe, was an artifact of the incomplete subtraction of the internal background. The prompt (veto2-bin: 650–800) and long-lived background "flux" spectra are plotted in figure VII.4. The prompt background dominates above 2 MeV. The long-lived component dominates the 1.2–1.8 MeV bin with a modest contribution to the 0.8–1.2 MeV bin. The veto2 rates of 650 and 2500 (the extreme values for the veto rates) correspond to cutoff-rigidities of approximately 15.5 and 4.5 GV, respectively. Adding the CDG flux reported here to the 4.5 GV (typical balloon environment) rigidity/veto dependent (prompt) background measured with COMPTEL yields flux values labeled as "COMPTEL flux ~ 4.5 GV" in figure VII.4 that agree with earlier measurements. Several CDG measurements were performed with detectors over Palestine (Texas) where the cutoff-rigidity is ~4.5 GV (e.g., White et al. 1977; Schönfelder et al. 1980). Therefore, scaling the COMPTEL flux to this ~4.5 GV cutoff-rigidity with no long-lived contributions accurately mimics the balloon environment used to perform the pre-COMPTEL CDG measurements. The balloon

experiments were short duration flights with no passage through the SAA, therefore we expect their long-lived background component to be low.

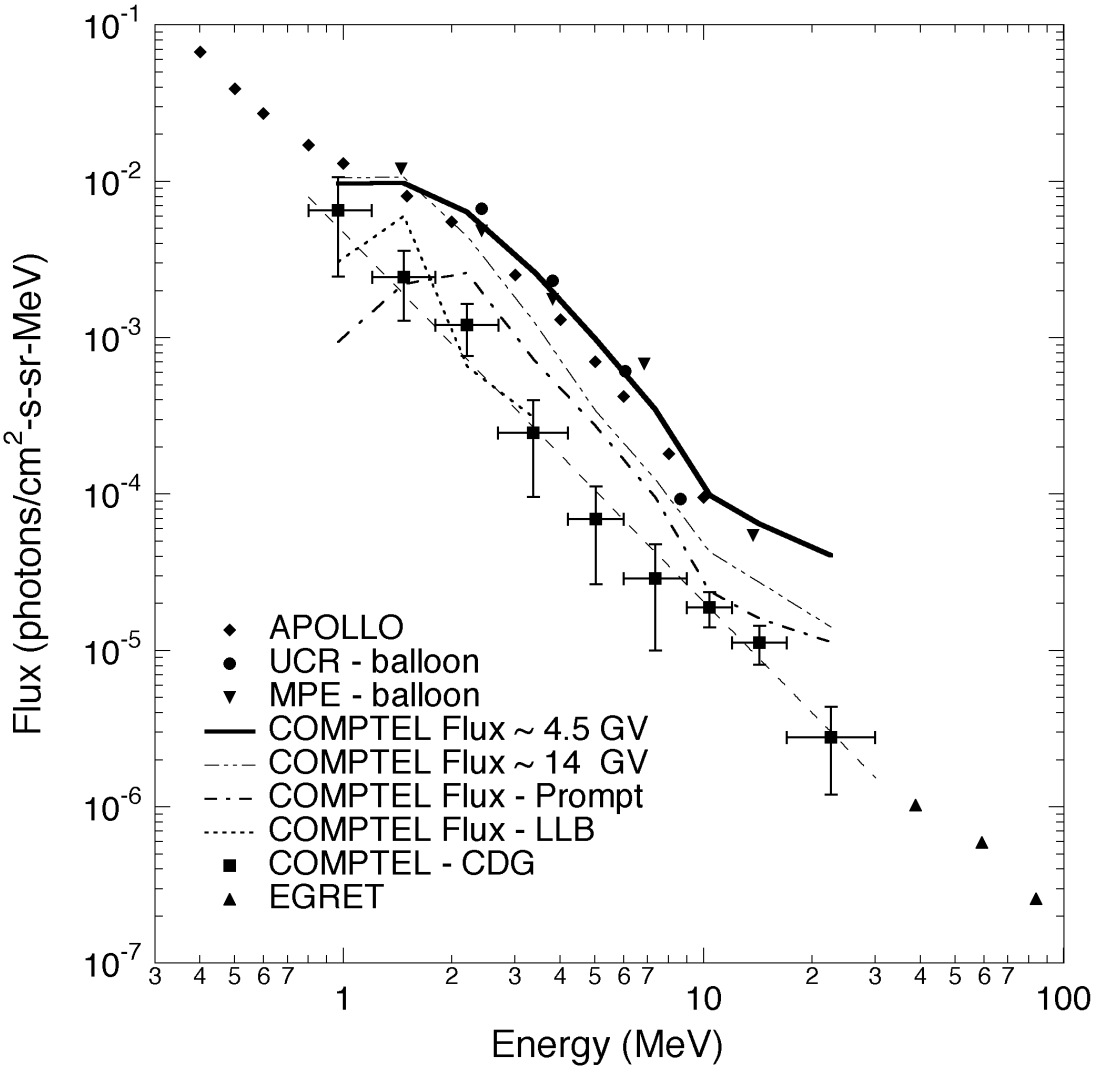

Figure VII.4 The COMPTEL flux at ~ 4.5 GV together with the pre-COMPTEL measurements. Also plotted is the COMPTEL flux at ~ 14 GV and the flux contributions from the prompt and long-lived background components.

Measurements of the CDG flux from balloons were made by extrapolating the downward moving gamma-ray flux measured at different float altitudes to zero g/cm^2 of atmosphere above the detector. The goal was to eliminate the downward moving atmospheric photon component that varies with atmospheric depth. However the Earth's albedo neutron flux is almost constant at the top of the atmosphere (above the Pfotzer maximum) (Preszler, Simnett, and White 1974). Therefore, the extrapolation to zero atmosphere does not remove the effects

of the constant neutron induced background, although White et al. (1977) and Schönfelder et al. (1980) attempted to correct for it.

Hence, the ability to extrapolate COMPTEL data to a zero cosmic-ray environment by extrapolating to zero charged-particle flux, corrects for cosmic-ray and neutron-induced prompt background and lowers the COMPTEL CDG flux values with respect to earlier measurements. Strictly speaking, the explanation for the MeV bump is valid only for the previous Compton telescopes. We present only a qualitative explanation, since the exact background in the UCR and MPE balloon experiments will depend on its mass distribution and the specific cosmic-ray environment during the measurements.

VII.D. Homogeneity of the CDG Emission

Time variability

The 9–30 MeV CDG flux was measured during five independent observations. The fluxes from these observations are listed in table VII.3 and are plotted in the figure VII.5 (statistical errors only). To test the hypothesis of a constant CDG emission, the five independent measurements were compared to the average value derived from the combined dataset, $(6.3 \pm 0.9) \times 10^{-6}$ (1/cm^2-s-sr-MeV). The reduced chi-square of the fit is 1.26. The null hypothesis of a constant flux is rejected only at only the 70% confidence level. Therefore, the COMPTEL 9–30 MeV flux measurements are consistent with a constant CDG emission.

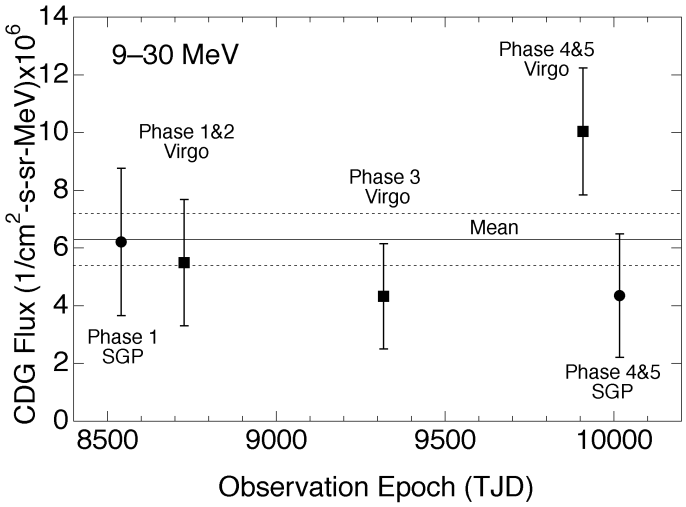

Figure VII.5 Five independent measurements of the 9–30 MeV CDG flux. The mean value and its 1σ range are also plotted.

Table VII.3 Five independent measurements of the 4.2–9 and 9–30 MeV CDG flux (statistical errors only, †2σ upper-limit).

Data	4.2–9 MeV CDG Flux $x10^{-5}$ (photons/cm^2-s-sr-MeV)	9–30 MeV CDG Flux $x10^{-6}$ (photons/cm^2-s-sr-MeV)
Virgo+SGP	4.3 ± 1.2	6.3 ± 0.9
Virgo	4.7 ± 1.5	6.8 ± 1.2
SGP	2.5 ± 2.2	4.7 ± 1.6
P12V	4.9 ± 2.6	5.5 ± 2.2
P3V	5.34†	4.3 ± 1.8
P45V	4.4 ± 2.9	10.0 ± 2.2
P1SGP	6.74†	6.2 ± 2.6
P45SGP	4.8 ± 2.9	4.3 ± 2.1

We performed the same test in the 4.2–9 MeV band. These fluxes are listed in table VII.3 and are plotted in the figure VII.6 (statistical errors only). The five independent 4.2–9 MeV measurements were compared to the average value derived from the combined dataset, $(4.3 \pm 1.2) \times 10^{-5}$ (1/cm^2-s-sr-MeV). The reduced chi-square of the fit is 0.04. The null hypothesis of a constant flux is rejected at only the 5% confidence level. Therefore, the COMPTEL 4.2–9 MeV flux measurements are also consistent with a constant CDG emission.

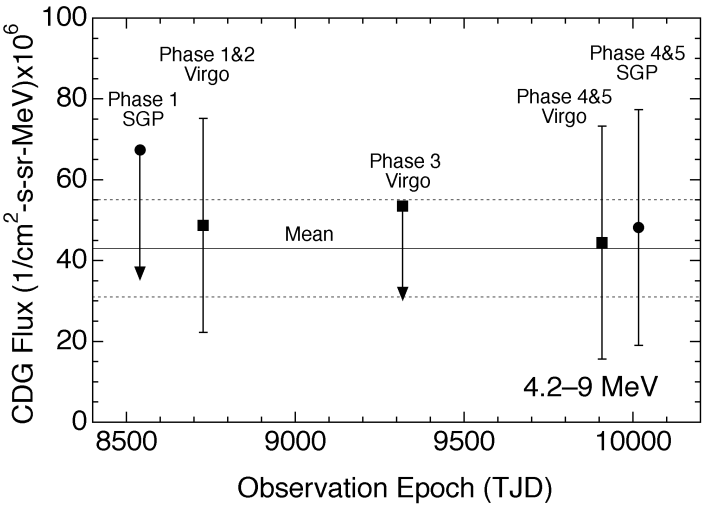

Figure VII.6 Five independent measurements of the 4.2–9 MeV CDG flux. The mean value and its 1σ range are also plotted.

Pointing variability

The observed Virgo and SGP regions represent large areas towards the North and South Galactic Poles. The measured CDG emission from these polar directions can be inspected for any large scale differences. The measured CDG spectrum above 4.2 MeV from the Virgo and SGP directions are plotted in figure VII.7 (statistical errors only) together with the power-law

fit to the total COMPTEL CDG spectrum. The spectrum from the Virgo and SGP directions are consistent with one another (see table VII.4).

Table VII.4 The CDG flux above 4.2 MeV from the Virgo and SGP directions (statistical errors only; $^{\dagger}2\sigma$ upper-limit).

Energy (MeV)	Virgo flux ($1/cm^2$-s-sr-MeV)	SGP flux ($1/cm^2$-s-sr-MeV)
4.2–6	$(7.0 \pm 3.0) \times 10^{-5}$	$(4.8 \pm 4.2) \times 10^{-5}$
6–9	$(3.2 \pm 1.6) \times 10^{-5}$	$6.3 \times 10^{-5\,\dagger}$
9–12	$(1.8 \pm 0.5) \times 10^{-5}$	$(1.7 \pm 0.6) \times 10^{-5}$
12–17	$(1.1 \pm 0.3) \times 10^{-5}$	$(8.0 \pm 3.5) \times 10^{-6}$
17–30	$(3.3 \pm 1.3) \times 10^{-6}$	$4.6 \times 10^{-5\,\dagger}$

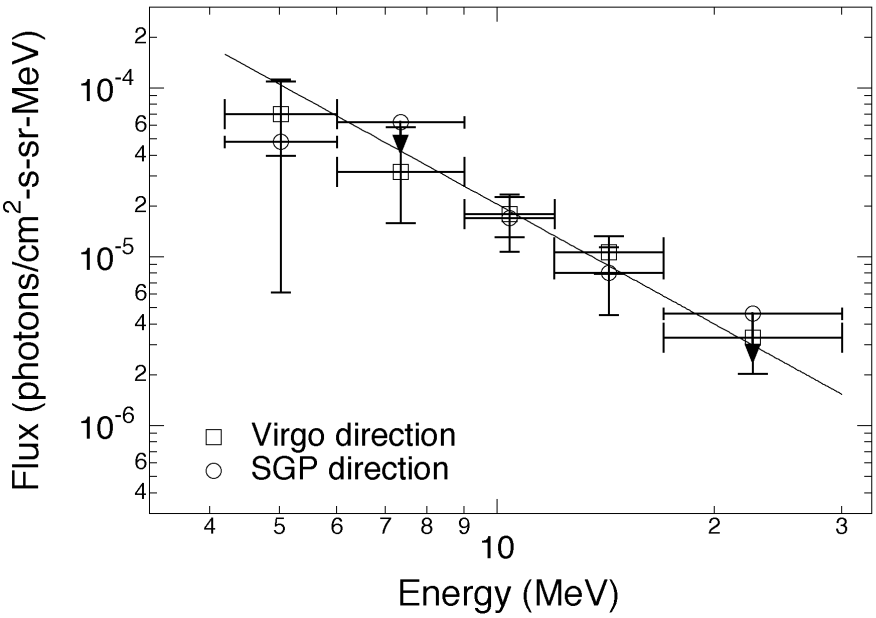

Figure VII.7 A comparison of the CDG spectrum for the Virgo and SGP observations together with the 0.8–30 MeV power-law fit.

Isotropy

The X-ray diffuse radiation from 5–100 keV is measured to be isotropic on scales larger than about 10˚ (Shafer and Fabian 1983). The degree of isotropy is not as well known in the gamma-ray regime. The SAS-2 results show uniformity over large scales (Fichtel, Simpson, and Thompson 1978). Recent results from the EGRET instrument show that the extragalactic emission is isotropic to within 20% of the flux measured in 36 separate regions of the sky (Sreekumar et al. 1998).

The ratio of the CDG flux from the SGP direction to that from the Virgo direction are computed and shown in table VII.5. Although not obvious in figure VII.7, the flux ratios are

0.53 ± 0.45 and 0.69 ± 0.26 for the 4.2–9 and 9–30 MeV ranges, respectively. The flux ratio for the combined 4.2–30 MeV range is 0.65 ± 0.23. Although the SGP intensity is lower in both energy ranges, the difference is significant at only $\sim 1.5\sigma$. Over large scales (Virgo and the South Galactic Pole), the 4.2–30 MeV CDG measurements are compatible with an isotropic emission to within 50% of the measured flux. A more detailed study of the granularity of the CDG emission is in progress [see Weidenspointner 1998].

Table VII.5 The 4.2–9 and 9–30 MeV CDG flux ratios from the Virgo and SGP directions (statistical errors only).

Data	4.2–9 MeV CDG Flux $x10^{-5}$ (photons/cm^2-s-sr-MeV)	9–30 MeV CDG Flux $x10^{-6}$ (photons/cm^2-s-sr-MeV)
Virgo	4.7 ± 1.5	6.8 ± 1.2
SGP	2.5 ± 2.15	4.68 ± 1.6
ratio	0.53 ± 0.45	0.69 ± 0.26

VII.E. Discussion

A variety of explanations for the origins of the diffuse extragalactic radiation have been proposed over the years. They include contributions from active galaxies, normal galaxies, matter-antimatter annihilation, supernovae emission, primordial black holes, etc. Many are relevant to the 1–30 MeV region and have been reviewed by others (see, for example, Fichtel and Trombka 1981; Gehrels and Cheung 1995; Silk 1973). Many have fallen out of favor due to improvements in the measurements or due to closer scrutiny of their predictions (Fichtel, Simpson, and Thompson 1978; Fichtel and Trombka 1981; Fichtel and Trombka 1997).

Rather than being a single source or mechanism, the high-energy diffuse radiation may well be composed of a number of different components, each with its own origin and contributions to specific energy ranges. Models discussing the diffuse origin are broadly classified into two groups: those that have a truly diffuse origin and those that are the superposition of unresolved sources.

Among the diffuse source models, the integrated emission from matter-antimatter annihilations in the context of a baryon-symmetric Universe has been proposed to explain the CDG emission between 1 and 100 MeV (Stecker 1971). Such a model was used to explain the MeV bump measured in the pre-COMPTEL MeV CDG spectrum. In the light of this work,

the contribution from such a process, if any, is significantly lower than previously believed. This model is further discussed in the following sections.

Active galaxies have long been postulated to be possible contributors to the high-energy diffuse radiation (Bignami et al. 1979). The EGRET team has reported the detection of over 60 AGNs (Hartmann et al. 1997), most of which are associated with flat-spectrum radio quasars or BL Lac objects and are usually referred to as *blazars*. They exhibit strong variability in many wavelengths and often show strong optical polarization or superluminal motion. However, only eight of the EGRET blazars have been detected by COMPTEL (Hartmann et al. 1997). The blazars detected by COMPTEL are also variable and show spectral breaks in the MeV energy range. Presently, active galaxies are considered to be the a likely source of the diffuse extragalactic radiation, with Seyferts contributing to the low energy (2–500 keV) regime and blazars dominating the high energy (>100 MeV) regime. Due to the small number of AGNs detected in the 1 to 30 MeV range, their contribution to the CDG emission at MeV energies in tentative. The integrated emission from Type Ia Supernovae is another unresolved source model that could contribute to the CDG radiation in the 300 keV to 2 MeV region (The, Leising, and Clayton 1993).

The multiwavelength spectrum of the CDG emission from low-energy X-rays to high energy gamma rays is shown in figure VII.8. The high-energy power-law spectrum a break around 4 MeV (long-dashed) is the contribution from blazars (Sreekumar, Stecker, and Kappadath 1997; McNaron-Brown et al. 1995). The SN Ia contribution (The, Leising, and Clayton 1993) (dotted), Seyfert 1 (dot-dashed) and Seyfert 2 (dashed) (Zdziarski 1996) contributions and the steep-spectrum quasar contribution (Chen, Fabian, and Gendreau 1996) (dot-dot-dashed) are also shown. The solid line is the sum of all these components. The discrete source models involving gamma-ray emission from active galaxies are further discussed in the following sections.

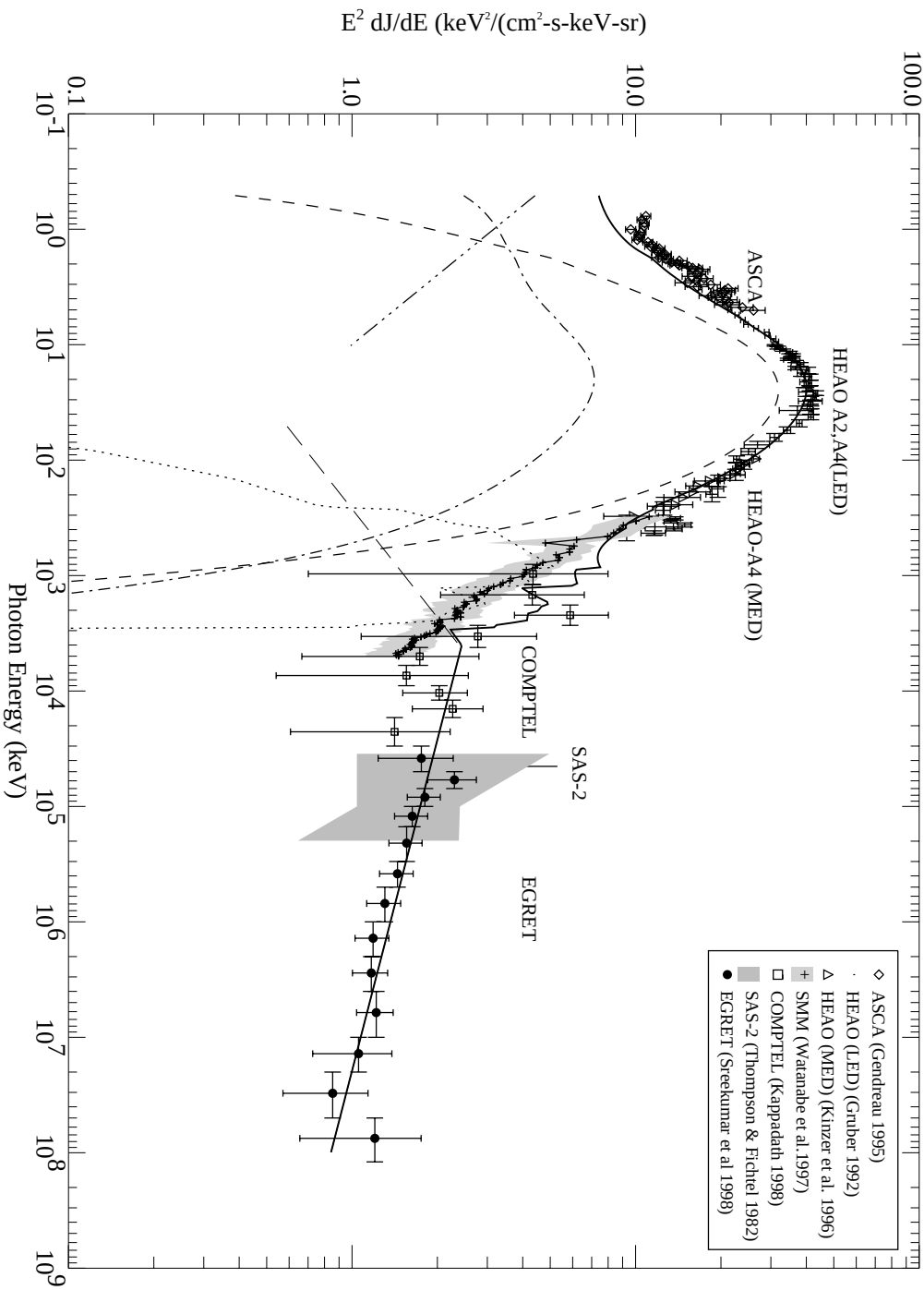

Figure VII.8 The multiwavelength spectrum of the CDG emission from low-energy X-rays to high-energy gamma rays. See text for an explanation of model components. Figure courtesy P. Sreekumar.

VII. E. 1 Matter-Antimatter Annihilation Radiation

Stecker et al. (1971; 1985) proposed a diffuse source model in which the CDG radiation in the 1–100 MeV region arises from matter-antimatter annihilations in a baryon-symmetric Universe. Within the framework of a baryon-symmetric Big-Bang cosmology (Omnès 1969), the early Universe separated into regions of matter and antimatter. These regions then evolved into large regions of matter and antimatter that now contain supercluster size masses. The matter-antimatter annihilation occurs at the boundaries of these regions producing the CDG radiation. To predict the gamma-ray spectrum it is necessary to solve the cosmological photon-transport equation as a function of redshift taking into account the energy loss from the pair-production and Compton-scattering processes.

The resulting gamma-ray spectrum is from the decay of π^0 mesons produced in proton-antiproton annihilation. The effects of Compton scattering and pair-production become only important at high redshifts (z >100) and result in the flattening of the spectrum below ~1 MeV. The characteristic features of this annihilation spectrum are a peak near 1 MeV, an approximate power law in the 5–100 MeV region above which the spectrum steepens with a cutoff at ~1 GeV (Stecker 1971).

The 1 MeV feature is essentially the redshifted π^0-decay spectrum, where the rest frame π^0-decay spectrum peaking at ~68 MeV is redshifted to 1 MeV (z~100). The most encouraging aspect of this model was the apparent explanation for the MeV bump present in the pre-COMPTEL CDG spectrum. There is now no evidence for a MeV bump so the annihilation spectrum is not required to the explain CDG emission near 1 MeV. Although there may be additional source components (e.g., from blazars), the extragalactic spectrum measured with EGRET indicates a power-law form from 30 MeV to 100 GeV, well above the maximum cutoff at ~1 GeV predicted by the annihilation model. The recent improvements in the CDG measurement above 1 MeV, the contribution from the matter-antimatter annihilation model, if any, is significantly lower than previously believed.

More importantly, it was argued that the presence of the MeV bump was experimental evidence for the existence of cosmological antiprotons (Stecker 1985). Other experimental evidence comes from examining the ratio of antiprotons to protons in cosmic rays. The latest measurements of antiprotons in cosmic rays are satisfactorily explained as secondary

products of cosmic-ray interactions with the interstellar medium (Streitmatter 1995). Therefore, at present, there is no compelling experimental evidence for the existence of cosmological antimatter, at least over large scales.

VII. E. 2 Active Galaxies

Seyferts Galaxies

The average Seyfert galaxy spectrum using data from the OSSE and Ginga experiments is characterized by an exponentially falling continuum (*e*-folding energy between 200–400 keV) together with a Compton-reflection component mainly below ~50 keV (Zdziarski et al. 1995). However no Seyfert galaxy has been detected above 1 MeV (Johnson et al. 1994; Maiscak et al. 1995). Therefore, although the Seyfert galaxies may explain a substantial fraction of the X-ray background (Zdziarski et al. 1996; Setti 1990), they are not expected to contribute to the diffuse radiation above ~500 keV (see figure VII.8).

Gamma ray emission has been observed from 50 keV to 1 GeV from a nearby radio galaxy Centaurus A (Steinle et al. 1998). Centaurus A is viewed from the side (~70˚) of the jet axis and has been classified as a Seyfert 2 object. It is the only Seyfert 2 galaxy seen above 1 MeV. If the emission from Centaurus A is typical for all Seyfert galaxies, in that, they all emit broadband emission in high-energy gamma rays at large angles with respect to the jet axis, then perhaps the integrated emission from Seyferts could be a substantial component to the CDG emission above 1 MeV and perhaps extending to 1 GeV.

Blazars

A simple calculation to illustrate the importance of the integrated gamma-ray emission from the 60 detected AGNs to the extragalactic diffuse flux: Sreekumar et al. (1998) measured an integral flux of 1.24×10^{-5} photons/cm^2-s-sr for the CDG emission above 100 MeV. Assuming a mean constant flux (>100 MeV) of $2–4\times10^{-7}$ photons/cm^2-s for all 60 detected blazars, their total intensity in the 10 sr outside the Galactic plane implies a flux of $1.2–2.4\times10^{-6}$ photons/cm^2-s-sr or 10–20% of the extragalactic flux.

Above 100 MeV, the blazar origin is also supported by the similarity between the diffuse extragalactic spectral index –2.10 ± 0.03 (Sreekumar et al. 1998) and the average blazar spectral index –2.15 ± 0.04 (Mukherjee et al. 1997). Since a standard cosmological

integration of a power-law source in energy results in the same spectral slope for its integrated emission, the similarity between the spectral indices for the blazars and the extragalactic diffuse emission is important.

Chiang et al. (1995) used the gamma-ray data of 33 blazars to deduce their gamma-ray luminosity function. By integrating this luminosity function over redshift, they showed that the bulk of the diffuse radiation above 100 MeV can be explained by unresolved gamma-ray-emitting AGNs. By applying the luminosity evolution obtained from radio data to gamma-ray blazars, other authors have estimated the contributions from blazars to the diffuse radiation above 100 MeV (e.g., Padovanni et al. 1993; Setti and Woltjer 1994; Stecker, Salamon, and Malkan 1993). These estimates agree with the intensity of the diffuse radiation. The uncertainties in all these calculation vary from ~25% to a factor of 2. However some authors have questioned the degree and nature of the correlation between the radio and gamma-ray luminosity for these blazars (Mücke et al. 1997).

The gamma-ray luminosity evolution function and the gamma-ray duty cycle are two major uncertainties in the blazar models for the diffuse radiation. The evolution described by Chiang et al. (1995) is consistent with that seen at radio frequencies making the ambiguities in the luminosity function less of a problem. Most blazars, however, show strong variability in their gamma-ray emission. For example, 3C 279 has varied by a factor of ~5 over the time scale of days with no significant change in the spectral index (Kniffen et al. 1993).

Although the blazar origin seems likely above ~100 MeV, the situation is less certain in the 1–30 MeV range. To date only eight of the EGRET blazars have been detected by COMPTEL (Hartmann et al. 1997). The blazars detected by COMPTEL are also variable and show spectral breaks in the MeV energy range. McNaron-Brown et al. (1995) have analyzed the multiwavelength spectra of the six blazars detected with OSSE, COMPTEL and EGRET. Using this limited dataset the “average” blazar spectrum is a power law with a spectral index of –2.15 that breaks at ~4 MeV and has a spectral index of –1.7 below it (Sreekumar, Stecker, and Kappadath 1997; McNaron-Brown et al. 1995). This average blazar spectrum is not in conflict with the COMPTEL results (see figure VII.8). However, caution is advised as six

blazars may not be representative of the overall blazar behavior due to possible selection effects.

COMPTEL has also detected a separate class of 2 identified blazars (Bloemen et al. 1995; Blom et al. 1995) and 3 unidentified sources (Collmar 1996; Iyudin et al. 1996; Williams et al. 1995) with narrow peaks at MeV energies, usually referred to as *MeV-blazars*. Although their global properties are not well known, the MeV-blazars could potentially contribute to the CDG emission (Comastri, Girolamo, and Setti 1996).

If one accepts the hypothesis that the CDG radiation is the sum of all blazar emission, then the CDG spectrum implies that the average blazar spectrum extends to ~100 GeV (Sreekumar, Stecker, and Kappadath 1997). The measured spectra of the individual blazars only extends to a few GeV because the intensity is too low to be measured at higher energies. In this context, we plot the COMPTEL CDG fluxes in the 4.2–9 MeV and 9–30 MeV range and compare it to the extrapolation of the EGRET CDG spectrum (see figure VII.9). The blazars detected by COMPTEL and OSSE usually have a break in the spectrum around a few MeV (McNaron-Brown et al. 1995). Although not inconsistent, the COMPTEL fluxes are systematically lower than the blazar component as shown in figure VII.9. If the CDG spectrum represents the average blazar spectrum, then the COMPTEL data, at face value, suggest that the average blazar spectrum changes smoothly ($\Delta\alpha < 0.4$) with a break between 30 and 100 MeV. A smooth change in the average blazar spectrum is not unexpected since the integration over redshift will tend to smooth out any breaks.

Stecker and Salamon (1996) have incorporated variability by considering quiescent and flare states for blazar emission in their calculation of the blazar contribution to the diffuse radiation. The flare-state blazars are taken to be harder than the quiescent-state blazars. Their calculations show a continuous hardening in the predicted diffuse spectrum. The predicted intensity for the CDG emission by their model (in keV^2/cm^2-s-sr-keV) is shown (rough estimate) in figure VII.9. The measured CDG spectrum shows no significant curvature. The model overpredicts the measurements below 50 MeV and above a few GeV.

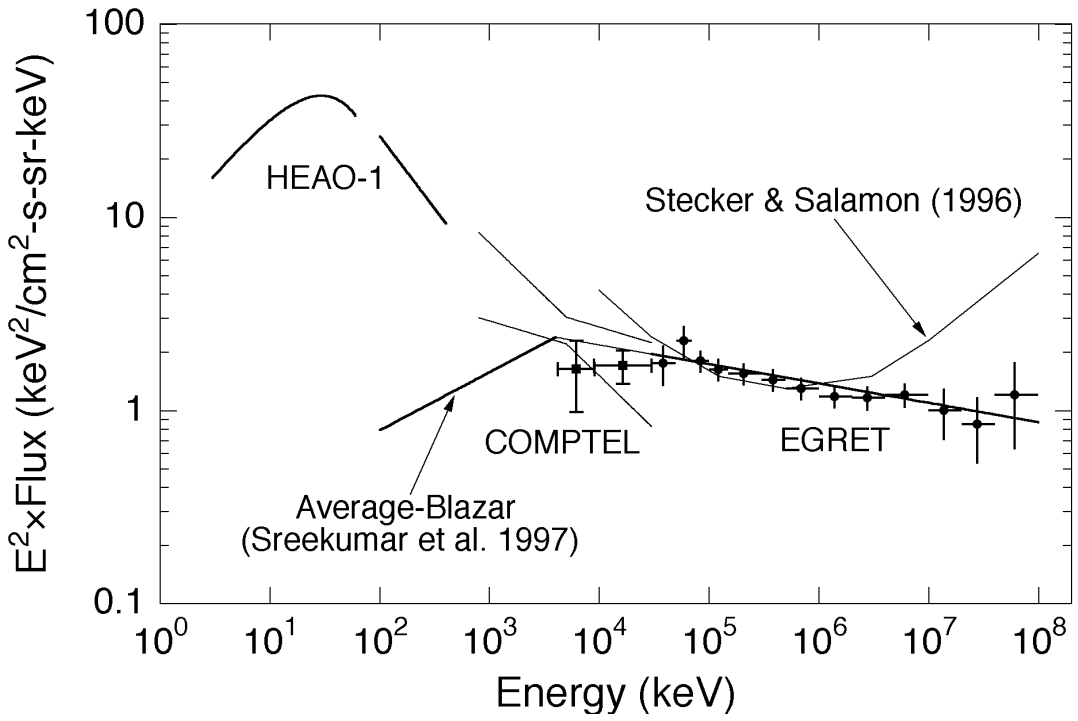

Figure VII.9 The E^2×Flux spectrum COMPTEL values from 4.2–30 MeV and EGRET values from 30 MeV to 100 GeV.

The curvature in the integrated spectrum arises from quiescent-state blazars with a steeper spectrum contributing to the lower energies (<500 MeV) and flare-state blazars with a harder or flatter spectrum contributing to the higher energies. There are some indications in the EGRET observations for a harder spectrum for some blazars in the flare-state (Mukherjee et al. 1996; Sreekumar et al. 1996). If both these hypotheses are true, then the COMPTEL measurements below 30 MeV and the EGRET measurements above a few GeV can serve as an important constraint for the ratio of quiescent to flare state blazar contribution to the CDG emission.

Normal Galaxies

Normal Galaxies like our own are known to emit gamma rays over a wide range of energies (from 500 keV to >50 GeV) and could also contribute to the diffuse radiation. Calculations by several researchers (Bignami et al. 1979; Setti and Woltjer 1994) have shown the intensity above 100 MeV from normal galaxies to be of order ~10% of the observed extragalactic emission.

VII. E. 3 Supernovae Contributions

The integrated emission from Type Ia Supernovae could also contribute significantly to the CDG radiation in the 300 keV to 2 MeV region (The, Leising, and Clayton 1993; Clayton, Colgate, and Fishman 1969). The reaction chain $^{56}Ni \rightarrow {}^{56}Co \rightarrow {}^{56}Fe$ produces gamma-ray lines at 0.847, 1.238, 1.770, 1.030, 2.599 and 3.250 MeV in the SNIa emission. There is also gamma-ray line emission from the decay of ^{26}Al, ^{44}Ti and ^{60}Co. Type Ia SNs are much brighter in gamma rays than Type II SNs partly because the massive envelopes in Type II SNs do not allow many of the gamma rays to escape. The Type II contribution is expected to be <5% (Watanabe et al. 1997; The, Leising, and Clayton 1993).

The et al. (1993) computed the cumulative SNIa contribution to the CDG radiation by integrating over time (or redshift) the number of continuum and line photons produced per ^{56}Fe decay from a standard Type Ia deflagration model. The important parameter in their calculation is the evolution function for the rate of nucleosynthesis. They performed calculations for a constant and an exponentially decreasing nucleosynthesis rate, with a turn-on time around $z = 2.5$. The results of both nucleosynthesis rates show that a large fraction of the CDG radiation between 0.3–2 MeV may be due to Type Ia SNs with a maximum cutoff at ~3 MeV. More recent calculations by Watanabe et al. (1997) taking into account the contributions from Type II SNs and using a star formation rate based on chemical evolution studies agree with the results of The et al. (1995).

The COMPTEL measurements below 3 MeV within errors are consistent with the level predicted by The et al. (1995). However much finer energy binning is required to examine spectral features such as edges near the line energies as predicted by this model that in turn may provide valuable constraints on the gamma-ray emission due to supernovae.